

# Quantum gravity of dust collapse

Viqar Husain,<sup>\*</sup> Jarod George Kelly,<sup>†</sup> Robert Santacruz,<sup>‡</sup> and Edward Wilson-Ewing<sup>§</sup>  
*Department of Mathematics and Statistics, University of New Brunswick, Fredericton, NB, Canada E3B 5A3*

We study the quantum gravitational collapse of spherically symmetric pressureless dust. Using an effective equation derived from a quantization in connection-triad phase space variables of general relativity, we find numerically, for a variety of initial dust configurations, that (i) trapped surfaces form and disappear as an initially collapsing density profile evolves into an outgoing shockwave; (ii) black hole lifetime is proportional to the square of its mass; and (iii) there is no mass inflation at inner apparent horizons. These results provide a substantially different view of black hole formation and subsequent evolution than found from a semi-classical analysis.

In classical general relativity, black holes are the final state of the gravitational collapse of sufficiently massive initial configurations of matter. Hints of the stability of black holes first appeared in linear stability analyses of black hole space-times, and subsequently through analytical [1] and numerical studies [2] of scalar field collapse in spherical symmetry.

In semiclassical gravity, defined broadly as the study of quantum test fields on curved space-time, it was discovered that black holes radiate [3] and therefore have a finite lifetime. The effect of this radiation on the black hole space-time is usually modelled by a sequence of quasi-static configurations of shrinking mass  $M(t)$ . Since Hawking radiation is that of a black body, at least to a first approximation, mass loss is described by the Stefan-Boltzmann law together with the facts that black hole mass is proportional to its radius, and its temperature is inversely proportional to mass. This leads to a black hole lifetime proportional to the cube of its mass in Planck units. Thus while black holes are stable in classical gravity, they are not in the semiclassical regime.

The lifetime result assumes that semiclassical gravity holds up to the final stages of black hole evaporation. However, since a black hole gets hotter and the curvature at the horizon gets larger as its mass shrinks, the semiclassical approximation is expected to fail at least in the late stages of evaporation due to the “backreaction” of Hawking radiation on the space-time, beyond just the effect due to shrinking mass.

What is required for a complete understanding of black hole physics is nothing less than a unified description of gravitational collapse in quantum gravity that is capable of describing the entire evolution, from the initial stages of collapse to the late stages of Hawking radiation and subsequent evolution of matter and space-time. Such an understanding might arise from the quantization of a classical model such as pressureless dust or scalar field in spherical symmetry.

There are a variety of studies that use spherically symmetric models with the ultimate aim of understanding the entire collapse process and subsequent evolution quantum mechanically. These fall into two main types, those that start from a black hole space-time, quantize

its interior as a cosmological space-time, and then match it to an exterior Schwarzschild metric [4–9], and those that avoid such an interior-exterior separation (and do not assume a pre-existing horizon) [10–21]. The work we present here falls in the second category.

In this Letter we develop and study an effective quantum gravity formalism for pressureless dust collapse in spherical symmetry. Classically this is the well-studied Lemaître-Tolman-Bondi (LTB) space-time; for earlier work towards a quantum theory of this model see [22–24]. We derive effective quantum-gravity corrected equations in the connection-triad variables [25, 26] for Hamiltonian general relativity, and solve them numerically for two classes of initial data.

Our main result is that in-falling dust bounces when space-time curvature reaches the Planck scale, and forms an outgoing shock wave. When the shock wave reaches the Schwarzschild radius, the trapped region(s) formed during in-fall disappear. This feature rules out remnants, and realizes explicitly the heuristic ideas concerning formation and evolution of non-singular black holes discussed in the literature [11, 27, 28]. We calculate the lifetime  $T$  of a black hole, and find  $T \sim M^2$ , a time much shorter than that predicted by Hawking radiation.

The class of metrics we study is

$$ds^2 = -dt^2 + \frac{(dx + N^x(x,t)dt)^2}{1 + \mathcal{E}(x,t)} + x^2 d\Omega^2, \quad (1)$$

where  $t \in \mathbb{R}$ ,  $x \in \mathbb{R}_{\geq 0}$  and  $d\Omega^2$  is the unit sphere metric. This is a Painlevé-Gullstrand form of the spherically symmetric Lemaître-Tolman-Bondi (LTB) space-times. The stress-energy tensor for dust is  $T_{ab} = \rho(x,t) u_a u_b$  where  $u^a$  is the unit 4-velocity of the dust field and  $\rho(x,t)$  its energy density.

Spherically symmetric metrics may be written in variables appropriate for the triad-connection phase space of general relativity. The (densitized) triads are defined by [19, 29]

$$E_1^x = E^a \sin \theta, \quad E_2^\theta = E^b \sin \theta, \quad E_3^\phi = E^b, \quad (2)$$

and give the metric

$$ds^2 = -N^2 dt^2 + \frac{(E^b)^2}{E^a} (dx + N^x dt)^2 + E^a d\Omega^2. \quad (3)$$

The corresponding Hamiltonian theory is given by the canonically conjugate phase space variables  $(a, E^a)$  and  $(b, E^b)$ , and the canonical pair corresponding to pressureless dust  $(T, p_T)$ . These satisfy the Poisson bracket relations

$$\begin{aligned} \{a(x), E^a(x')\} &= 2G\gamma \delta(x - x'), \\ \{b(x), E^b(x')\} &= G\gamma \delta(x - x'), \\ \{T(x), p_T(x')\} &= \delta(x - x')/4\pi, \end{aligned} \quad (4)$$

where  $\gamma$  is the Barbero-Immirzi parameter. These variables are subject to the Hamiltonian and diffeomorphism constraints of general relativity. We fix the gauge freedom generated by the first constraint by setting  $T = t$  [30], and the second by setting  $E^a = x^2$ . Preservation of these gauge-fixing conditions under evolution requires  $N = 1$  [20, 30] and  $N^x = -b/\gamma$  [12, 19]. The resulting Hamiltonian theory has one remaining local degree of freedom with phase space variables  $(b, E^b)$ . The reduced canonical action is

$$S_{GF} = \int dt \int dx \left( \frac{\dot{b}E^b}{G\gamma} - \mathcal{H}_{\text{phys}} \right), \quad (5)$$

$$\mathcal{H}_{\text{phys}} \equiv -\frac{1}{2G\gamma} \left[ \frac{E^b}{\gamma x} \partial_x (x b^2) + \frac{\gamma E^b}{x} + \frac{2\gamma x^2}{(E^b)^2} \partial_x E^b - \frac{3\gamma x}{E^b} \right]. \quad (6)$$

$\mathcal{H}_{\text{phys}}$  is the true physical Hamiltonian. The dust energy density is

$$\rho = -\frac{\mathcal{H}_{\text{phys}}}{4\pi x E^b}, \quad (7)$$

and the total mass contained within a radius  $x$  is

$$m(x, t) = 4\pi \int_0^x d\tilde{x} \tilde{x} E^b \rho = -\int_0^x d\tilde{x} \mathcal{H}_{\text{phys}}. \quad (8)$$

This completes the description of the classical theory.

We quantize the theory by first defining a discretization of the classical theory on a radial lattice, a procedure similar in spirit to lattice gauge theory. Let us define an equi-spaced radial lattice:  $x \rightarrow x_n, n = 0 \dots N$ , with  $x_{n+1} - x_n = w$ ,  $f_n = f(x_n)$ , and  $\partial_x f(x_n) \rightarrow (f_{n+1} - f_n)/w$ . The phase space variables are then defined at discrete points  $b_n(t) \equiv b(x_n, t)$  and  $E_n^b(t) \equiv E^b(x_n, t)$ , and their fundamental Poisson bracket is  $\{b_n, E_m^b\} = G\gamma \delta_{m,n}/w$ . The physical Hamiltonian  $\mathcal{H}_{\text{phys}}$  becomes a sum over lattice sites.

We quantize this discrete theory using a polymer quantization that proceeds by representing at each point  $n$  the algebra

$$\{\exp(i\mu b_n), E_n^b\} = \frac{i\mu G\gamma}{w} \exp(i\mu b_n) \quad (9)$$

on the Hilbert space  $\mathbb{H}_n$  with basis vectors  $|E^b\rangle_n$  and inner product  ${}_n \langle E^b | E^{b'} \rangle_n = \delta_{E^b, E^{b'}}$ ; this is similar to

the momentum representation for a particle on  $\mathbb{R}$  with the difference that the r.h.s. is the Kronecker delta. This discrete inner product is the defining feature of the polymer Hilbert space  $\mathbb{H}_n$ . With  $\mathcal{N}_n(\mu) \equiv \exp(i\mu b_n)$ , the representation is defined by

$$\begin{aligned} \hat{E}_n^b |E^b\rangle_n &= E^b |E^b\rangle_n, \\ \hat{\mathcal{N}}_n(\mu) |E^b\rangle_n &= |E^b + \hbar G\gamma \mu/w\rangle_n. \end{aligned} \quad (10)$$

The Hilbert space for the entire lattice is the tensor product  $\mathbb{H} = \otimes_{n=0}^N \mathbb{H}_n$ .

The operator corresponding to the Hamiltonian  $\mathcal{H}_{\text{phys}}$  requires a definition of the operator  $\hat{b}_n$  from the elementary operators (10). The simplest possibility is (see, e.g., [26])

$$\hat{b}_n(\mu) = \frac{1}{2i\mu} \left( \hat{\mathcal{N}}_n(\mu) - \hat{\mathcal{N}}_n(\mu)^\dagger \right). \quad (11)$$

The parameter  $\mu$  is as yet unspecified—it may be a constant, or a function of  $x_n$  and/or  $E_n^b$  without affecting the algebra. A physical ingredient is required to fix it. To do this, recall that since  $E^b$  is the  $\theta$  component of the triad,  $\mathcal{N}_n(\mu)$  is the generator of translations in the  $\theta$  direction by an angle  $\mu$ . The physical distance in this direction at the radial lattice point  $x_n$  is  $|\Delta s| = x_n \mu = \ell_{\text{Pl}}$ , where the last equality is the desired physical input: the elementary translation operator in the Hamiltonian should correspond to a Planck-length step. This sets [19]

$$\mu = \frac{\ell_{\text{Pl}}}{x_n}. \quad (12)$$

This summarizes the quantization; details appear in [31].

An effective Hamiltonian can be extracted from this quantization by replacing  $b_n$  in the discretized  $\mathcal{H}_{\text{phys}}$  by the corresponding classical function that contains Planck length corrections, and then taking the continuum limit. Using (11) and (12) this classical function is

$$\tilde{b}_n = \frac{x_n}{\ell_{\text{Pl}}} \sin \left( \frac{\ell_{\text{Pl}} b_n}{x_n} \right), \quad (13)$$

and the continuum limit gives

$$\begin{aligned} \mathcal{H}_{\text{phys}}^{\text{eff}} &= -\frac{1}{2G\gamma} \left[ \frac{E^b}{\gamma \ell_{\text{Pl}}^2} \partial_x \left( x^3 \sin^2 \left( \frac{\ell_{\text{Pl}} b}{x} \right) \right) \right. \\ &\quad \left. + \frac{2\gamma x^2}{(E^b)^2} \partial_x E^b - \frac{3\gamma x}{E^b} + \frac{\gamma E^b}{x} \right]. \end{aligned} \quad (14)$$

Setting  $\gamma = \ell_{\text{Pl}} = 1$ , the effective equations obtained from this Hamiltonian are

$$\dot{b} = \frac{x}{2E_b^2} - \frac{1}{2x} - x \sin \frac{b}{x} \left[ \frac{3}{2} \sin \frac{b}{x} + x \partial_x \sin \frac{b}{x} \right], \quad (15)$$

$$\dot{E}_b = -\frac{x^2}{2} \partial_x \left( \frac{E_b}{x} \right) \sin \frac{b}{x} \cos \frac{b}{x}. \quad (16)$$

It is evident that  $E^b = x$  is a solution of the second equation. In classical theory this corresponds to the class of LTB solutions with  $\mathcal{E}(x) = 0$  in the metric (1). In the remainder of this Letter, we consider this class of space-times. With  $E^b = x$ , the effective equation (15) simplifies,

$$\dot{b} + \frac{1}{2x} \partial_x \left( x^3 \sin^2 \frac{b}{x} \right) = 0. \quad (17)$$

To summarize our results to this point, after gauge-fixing the scalar and diffeomorphism constraints, we quantized the spherically symmetric pressureless dust model; from this we obtained the effective equations (15)-(16) containing Planck scale corrections; and lastly we restricted to the class of solutions of the effective equations with  $E^b = x$ , resulting in (17).

For the class of solutions with  $E^b = x$ , the energy density is related to  $b(x, t)$  by

$$\rho = -\frac{\mathcal{H}_{\text{phys}}^{\text{eff}}}{4\pi x^2} = \frac{1}{8\pi x^2} \partial_x \left( x^3 \sin^2 \frac{b}{x} \right), \quad (18)$$

and the effective metric is

$$ds^2 = -dt^2 + \left( dx + N^x(x, t) dt \right)^2 + x^2 d\Omega^2. \quad (19)$$

Recalling that  $N^x = -b$  is induced by the gauge-fixing condition  $E^a = x^2$ , we require an effective expression for  $N^x$  compatible with that used for  $b^2$  in  $\mathcal{H}_{\text{phys}}$  (6). This is

$$N^x = -\frac{x}{2} \sin \left( \frac{2b}{x} \right), \quad (20)$$

a form also used in related discussions of effective equations in vacuum spherical symmetry [18, 19].

To solve (17) numerically, we first define the variable  $B(x, t) = xb(x, t)$  to simplify (17) to the form of a conservation law, and then rewrite it as an integral equation so discontinuities in  $B$  can be handled, giving

$$\frac{d}{dt} \int_{x_1}^{x_2} B(x, t) dx + \frac{1}{2} \left[ x^3 \sin^2 \left( \frac{B(x, t)}{x^2} \right) \right]_{x_1}^{x_2} = 0; \quad (21)$$

the term in brackets is the mass function

$$m(x, t) = 4\pi \int_0^x r^2 \rho(r, t) dr = \frac{1}{2} x^3 \sin^2 \left( \frac{B}{x^2} \right). \quad (22)$$

Our numerical procedure is the well-known Godunov method (see, e.g., [32]). This method involves dividing the integration domain into cells, solving the Riemann problem in each cell, and enforcing flux continuity between cells. The only generalization of this method necessary for our purposes comes from noting that the current in the continuity equation (21) depends explicitly on position  $x$ ; we address this by evaluating  $x$  at the boundary between two cells when computing the flux.

To specify initial data we fix the mass function for a total mass  $M$  by defining

$$m_0(x) = M \frac{\int_0^x r^2 \rho_0(r) dr}{\int_0^\infty r^2 \rho_0(r) dr}. \quad (23)$$

Through (22), this determines the initial value  $B_0(x)$ . We use two types of initial density profiles with parameters  $(x_0, \sigma)$ , the Gaussian and the hyperbolic tangent functions

$$\rho_0^G(x) = \exp[-(x - x_0)^2 / \sigma^2], \quad (24)$$

$$\rho_0^T(x) = 1 + \tanh[-(x - x_0) / \sigma]. \quad (25)$$

The first is a smooth dust ring centred at  $x_0$ , and the second is a star-like distribution of near constant density and initial radius  $x_0$ . In both cases we set  $\sigma$  and  $x_0$  such that initially there is no apparent horizon.

At each time step we compute the density  $\rho(x, t)$  and the function

$$\begin{aligned} \Theta_+(x, t) &= |\nabla x|^2 = 1 - (N^x)^2 \\ &= 1 - \frac{x^2}{4} \sin^2 \left( \frac{2B}{x^2} \right), \end{aligned} \quad (26)$$

using the expression (20) for the effective  $N^x$ ; the zeros of this function determine the locations of apparent horizons, see, e.g., [33].

Figure 1 shows frames from the evolution of a linear combination of initial Gaussian data. Several features are evident: (i) during the collapse, apparent horizons form in pairs (located at the zeros of  $\Theta_+$ ), the first due to the closer profile, and subsequently the second; (ii) there is a bounce at the origin; (iii) an outgoing gravitational shock wave forms, and horizons eventually disappear as the shock wave moves outward; (iv) the density and mass function remain bounded at all times, and the total mass is conserved under evolution; (v) there is no instability or mass inflation (unlike in classical general relativity [34, 35]); (vi) after the inner profile bounces, its collision with the second ingoing profile does not result in recollapse; (vii) there is no curvature singularity. These features are observed in all our simulations, and are qualitatively independent of  $\sigma$  and  $x_0$ .

We computed the lifetime  $T$  of the black hole as a function of the total mass  $M$  of the data for the initial density configurations (24) and (25) by recording during the simulation the time interval (in Planck units) between the formation of the outermost apparent horizon and its disappearance. The results are shown in Figs. 2 and 3 (for  $\sigma = 1/2$ ). The linear dependence in the log-log plots is apparent. The fit to the curves appears in top left corners of these figures. The coefficient of  $M^2$  is approximately  $8\pi/3$ , a numerical factor that can be computed analytically for the quantum Oppenheimer-Snyder model [31]. Thus the leading order contribution to  $T$  is

$$T \sim \frac{8\pi}{3} M^2, \quad (27)$$

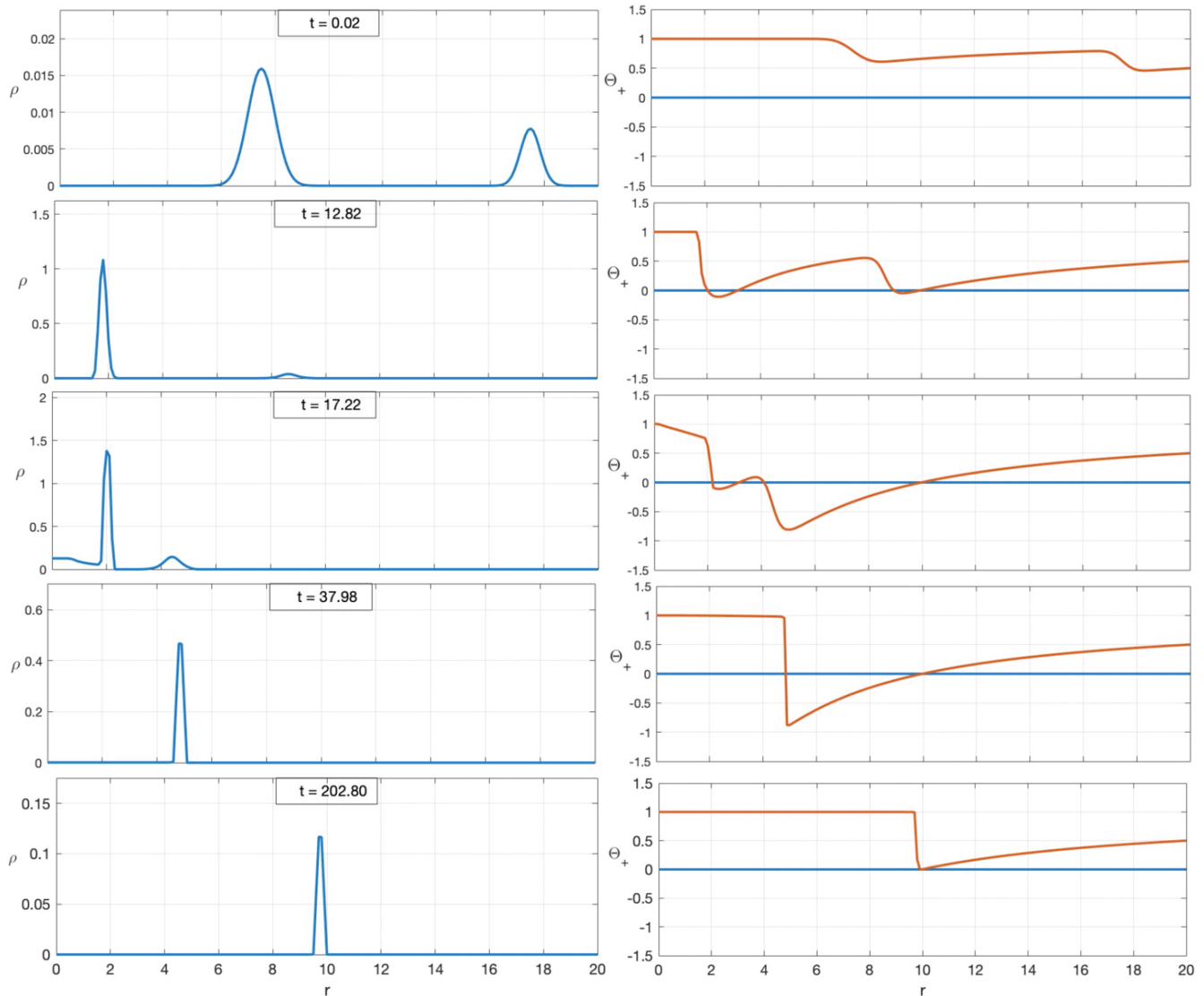


FIG. 1. Dust density  $\rho$  (left column) and apparent horizon function  $\Theta_+$  (right column) at the times indicated. The initial data is  $\rho_0(r) = \exp(-2(x - 1.5M)^2)/5 + \exp(-4(x - 3.5M)^2)/10$  with  $M = 5$  in (23). The first two rows show the ingoing dust, the middle one shows the bounce, and the last two show the outgoing shock wave until apparent horizons (the zeros of  $\Theta_+$ ) disappear at  $t \sim 202$ , in Planck units. For this initial data the outermost horizon forms at  $r = x = 2M = 10$ , and all mass falls within this radius before the bounce. (The vertical axes in the left column vary from one frame to the next.)

over three orders of magnitude in  $T$  for both initial data profiles.

To summarize, we derived effective Hamiltonian equations that describe quantum gravitational features of dust collapse in the loop quantum gravity formalism. Our approach is based on: (i) a complete gauge-fixing of the Hamiltonian and diffeomorphism constraints that gives a physical Hamiltonian, (ii) a discretization and quantization of this system in a polymer framework that includes a minimal length, and (iii) numerical integration of a subclass of the effective equations. We found numerically that black holes are transitory and non-singular,

with a lifetime proportional to the square of their mass to leading order.

A point of particular interest concerning our black hole lifetime result is its consequence for Hawking radiation: it would commence when the outermost apparent horizon forms, and cease when it disappears a time  $\sim M^2$  later. For  $M > 1$  in Planck units, this is shorter than the Page time [36], when Hawking radiation and black hole entropy are maximally entangled. Therefore it seems likely that the black hole information loss problem does not arise in the setting we have described. We leave an investigation of this and related questions for future work.

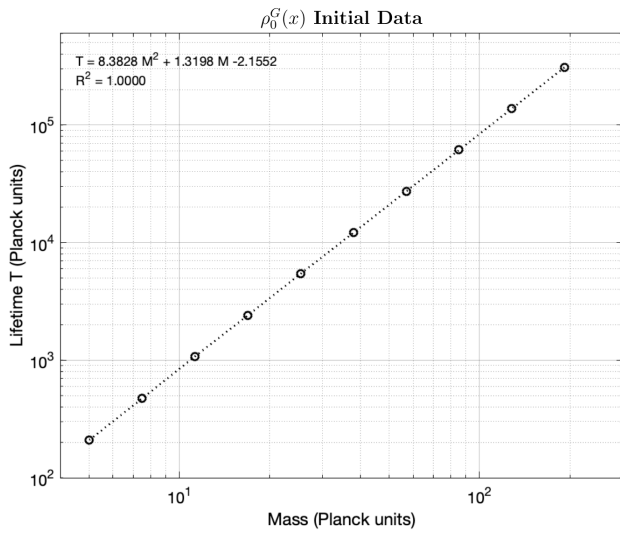


FIG. 2. Black hole lifetime for initial data (24) with  $\sigma = 0.5$ .

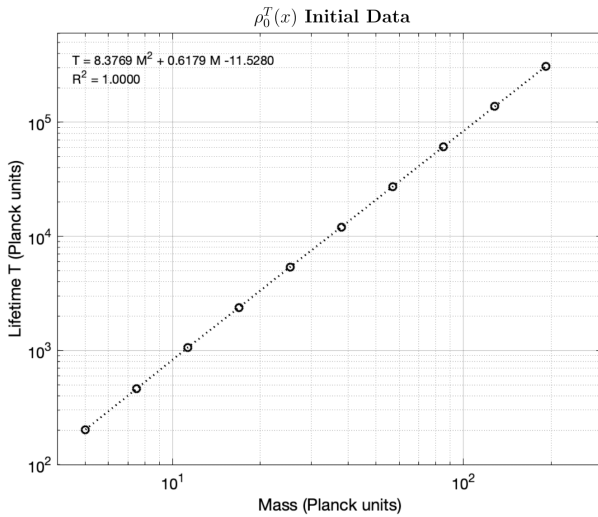


FIG. 3. Black hole lifetime for initial data (25) with  $\sigma = 0.5$ .

*Acknowledgements:* This work was supported by the Natural Sciences and Engineering Research Council of Canada. E.W.-E. also acknowledges support from the UNB Fritz Grein Award.

\* vhusain@unb.ca

† jarod.kelly@unb.ca

‡ robert.santacruz@unb.ca

§ edward.wilson-ewing@unb.ca

- [1] D. Christodoulou, “The Structure and Uniqueness of Generalized Solutions of the Spherically Symmetric Einstein Scalar Equations,” *Commun. Math. Phys.* **109** (1987) 591–611.

- [2] M. W. Choptuik, “Universality and scaling in gravitational collapse of a massless scalar field,” *Phys. Rev. Lett.* **70** (1993) 9–12.
- [3] S. W. Hawking, “Particle Creation by Black Holes,” *Commun. Math. Phys.* **43** (1975) 199–220. [Erratum: *Commun. Math. Phys.* **46**, 206 (1976)].
- [4] L. Modesto, “Semiclassical loop quantum black hole,” *Int. J. Theor. Phys.* **49** (2010) 1649–1683, [arXiv:0811.2196](#).
- [5] C. G. Boehmer and K. Vandersloot, “Loop Quantum Dynamics of the Schwarzschild Interior,” *Phys. Rev.* **D76** (2007) 104030, [arXiv:0709.2129](#).
- [6] R. Gambini and J. Pullin, “Loop quantization of the Schwarzschild black hole,” *Phys. Rev. Lett.* **110** (2013) 211301, [arXiv:1302.5265](#).
- [7] A. Corichi and P. Singh, “Loop quantization of the Schwarzschild interior revisited,” *Class. Quant. Grav.* **33** (2016) 055006, [arXiv:1506.08015](#).
- [8] A. Ashtekar, J. Olmedo, and P. Singh, “Quantum extension of the Kruskal spacetime,” *Phys. Rev.* **D98** (2018) 126003, [arXiv:1806.02406](#).
- [9] N. Bodendorfer, F. M. Mele, and J. Münch, “Effective Quantum Extended Spacetime of Polymer Schwarzschild Black Hole,” *Class. Quant. Grav.* **36** (2019) 195015, [arXiv:1902.04542](#).
- [10] V. Husain and O. Winkler, “Quantum black holes from null expansion operators,” *Class. Quant. Grav.* **22** (2005) L135–L142, [arXiv:gr-qc/0412039](#).
- [11] S. A. Hayward, “Formation and evaporation of regular black holes,” *Phys. Rev. Lett.* **96** (2006) 031103, [arXiv:gr-qc/0506126](#).
- [12] M. Campiglia, R. Gambini, and J. Pullin, “Loop quantization of spherically symmetric midi-superspaces,” *Class. Quant. Grav.* **24** (2007) 3649–3672, [arXiv:gr-qc/0703135](#).
- [13] S. Hossenfelder, L. Modesto, and I. Premont-Schwarz, “A Model for non-singular black hole collapse and evaporation,” *Phys. Rev.* **D81** (2010) 044036, [arXiv:0912.1823](#).
- [14] A. Kreienbuehl, V. Husain, and S. S. Seahra, “Modified general relativity as a model for quantum gravitational collapse,” *Class. Quant. Grav.* **29** (2012) 095008, [arXiv:1011.2381](#).
- [15] J. Ziprick and G. Kunstatter, “Dynamical Singularity Resolution in Spherically Symmetric Black Hole Formation,” *Phys. Rev.* **D80** (2009) 024032, [arXiv:0902.3224](#).
- [16] M. Bojowald, S. Brahma, and D.-h. Yeom, “Effective line elements and black-hole models in canonical loop quantum gravity,” *Phys. Rev.* **D98** (2018) 046015, [arXiv:1803.01119](#).
- [17] F. Benitez, R. Gambini, L. Lehner, S. Liebling, and J. Pullin, “Critical collapse of a scalar field in semiclassical loop quantum gravity,” *Phys. Rev. Lett.* **124** (2020) 071301, [arXiv:2002.04044](#).
- [18] R. Gambini, J. Olmedo, and J. Pullin, “Spherically symmetric loop quantum gravity: analysis of improved dynamics,” [arXiv:2006.01513](#).
- [19] J. G. Kelly, R. Santacruz, and E. Wilson-Ewing, “Effective loop quantum gravity framework for vacuum spherically symmetric spacetimes,” *Phys. Rev.* **D102** (2020) 106024, [arXiv:2006.09302](#).
- [20] J. G. Kelly, R. Santacruz, and E. Wilson-Ewing, “Black hole collapse and bounce in effective loop quantum



- gravity,” *Class. Quant. Grav.* **38** (2021) 04LT01, [arXiv:2006.09325](#).
- [21] M. Han and H. Liu, “Improved Effective Dynamics of Loop-Quantum-Gravity Black Hole and Nariai Limit,” [arXiv:2012.05729](#).
- [22] C. Vaz and L. Witten, “Canonical quantization of spherically symmetric dust collapse,” *Gen. Rel. Grav.* **43** (2011) 3429–3449, [arXiv:1111.6821](#).
- [23] M. Bojowald, T. Harada, and R. Tibrewala, “Lemaitre-Tolman-Bondi collapse from the perspective of loop quantum gravity,” *Phys. Rev.* **D78** (2008) 064057, [arXiv:0806.2593](#).
- [24] C. Kiefer and T. Schmitz, “Singularity avoidance for collapsing quantum dust in the Lemaître-Tolman-Bondi model,” *Phys. Rev.* **D99** (2019) 126010, [arXiv:1904.13220](#).
- [25] A. Ashtekar and J. Lewandowski, “Background independent quantum gravity: A Status report,” *Class. Quant. Grav.* **21** (2004) R53, [arXiv:gr-qc/0404018](#).
- [26] N. Bodendorfer, “An elementary introduction to loop quantum gravity,” [arXiv:1607.05129](#).
- [27] A. Ashtekar and M. Bojowald, “Black hole evaporation: A Paradigm,” *Class. Quant. Grav.* **22** (2005) 3349–3362, [arXiv:gr-qc/0504029](#).
- [28] C. Rovelli and F. Vidotto, “Planck stars,” *Int. J. Mod. Phys.* **D23** (2014) 1442026, [arXiv:1401.6562](#).
- [29] M. Bojowald and R. Swiderski, “Spherically symmetric quantum geometry: Hamiltonian constraint,” *Class. Quant. Grav.* **23** (2006) 2129–2154, [arXiv:gr-qc/0511108](#).
- [30] V. Husain and T. Pawłowski, “Time and a physical Hamiltonian for quantum gravity,” *Phys. Rev. Lett.* **108** (2012) 141301, [arXiv:1108.1145](#).
- [31] V. Husain, J. G. Kelly, R. Santacruz, and E. Wilson-Ewing, to appear.
- [32] R. J. LeVeque, *Finite Volume Methods for Hyperbolic Problems*. Cambridge Texts in Applied Mathematics. Cambridge University Press, 2002.
- [33] V. Faraoni, G. F. R. Ellis, J. T. Firouzjaee, A. Helou, and I. Musco, “Foliation dependence of black hole apparent horizons in spherical symmetry,” *Phys. Rev.* **D95** (2017) 024008, [arXiv:1610.05822](#).
- [34] D. M. Eardley, “Death of White Holes in the Early Universe,” *Phys. Rev. Lett.* **33** (1974) 442–444.
- [35] E. Poisson and W. Israel, “Inner-horizon instability and mass inflation in black holes,” *Phys. Rev. Lett.* **63** (1989) 1663–1666.
- [36] D. N. Page, “Average entropy of a subsystem,” *Phys. Rev. Lett.* **71** (1993) 1291–1294, [arXiv:gr-qc/9305007](#).